Journal of Applied Electrochemistry **30**: 1345–1350, 2000.

Oxidation of carboxylic acids at boron-doped diamond electrodes for wastewater treatment†

D. GANDINI[1], E. MAHÉ[1,3], P.A. MICHAUD[1], W. HAENNI[2], A. PERRET[2] and Ch. COMNINELLIS[1]*
[1]*Institute of Chemical Engineering, Swiss Federal Institute of Technology, CH-1015 Lausanne, Switzerland*
[2]*CSEM Centre Suisse d'Electronique et de Microtechnique S.A, Rue Jacquet-Droz 1, CH-2007 Neuchâtel, Switzerland*
[3]*On leave from UMR 7612 LI2C-CNRS-UPMC, 4 Place Jussieu, 75252 Paris Cedex 05, France*
*(*author for correspondence, e-mail: christos.comninellis@epfl.ch.)*

Received 23 July 1999; accepted in revised form 19 October 1999

Key words: boron-doped diamond electrodes, electrochemical oxidation, organics, wastewater treatment

Abstract

Thin boron-doped diamond films have been prepared by HF CVD (hot filament chemical vapour deposition technique) on conductive p-Si substrate (Si/Diamond). The morphology of these Si/diamond electrodes has been investigated by SEM and Raman spectroscopy. The electrochemical behaviour of the Si/diamond electrodes in 1 M H_2SO_4 and in 1 M H_2SO_4 + carboxylic acids has been investigated by cyclic voltammetry. Finally, the electrochemical oxidation of some simple carboxylic acids (acetic, formic, oxalic) has been investigated by bulk electrolysis. These acids can be oxidized at Si/diamond anodes to CO_2, in the potential region of water and/or the supporting electrolyte decomposition, with high current efficiency.

1. Introduction

Oxidative electrochemical processes promising versatility, environmental compatibility and cost effectiveness have a continuously growing importance both in selective organic synthesis and in degradation of organic pollutants. For the oxidative degradation of organics in wastewater treatment, the aim is the complete oxidation of organics to CO_2 [1–4] or the conversion of the toxic organics to biocompatible compounds [5, 6].

The electrode material is clearly an important parameter when optimizing such processes since the mechanism and the products of several anodic reactions are known to depend on the anode material. For example, the anodic oxidation of phenol yields hydroquinone and benzoquinone at Ti/IrO_2 anodes and mainly carbon dioxide at Ti/SnO_2–Sb_2O_5 anodes [7].

In previous work a generalized mechanism for the oxidation of organics in the potential region of O_2 evolution was proposed [8–10]. This mechanism explains the complete oxidation of organics to CO_2 by electrogenerated hydroxyl radicals on 'non-active' electrodes and the selective oxidation on 'active' electrodes. According to this mechanism, boron doped diamond, a 'non-active' electrode, is an ideal anode for the complete oxidation of organics to CO_2 for wastewater treatment.

The electrochemistry of synthetic boron-doped diamond films has received great attention recently [11–15]. Few electrochemical studies have been made on synthetic boron-doped diamond films with the goal of developing application in the electrochemical oxidation of organics for waste water treatment [16–18].

The results have shown that only reactions involving simple electron transfer are active on diamond electrodes in the potential region of water stability [17, 18]. For oxidation reactions with more complex mechanisms, complex oxidation reactions can take place on diamond electrodes only in the potential region of water discharge [17, 18]. Diamond electrodes have also been successfully used for the anodic oxidation of cyanide and the cathodic recovery of heavy metals [19].

Synthetic boron doped diamond films have also been successfully deposited on titanium base metal (Ti/diamond) [20]. The configuration of this electrode is similar to DSA (dimensionally stable anodes) electrodes and opens up new possibilities in industrial electrochemistry. It has been reported that the main reason for the successful preparation of the Ti/Diamond electrodes is the formation of a TiC interlayer between the Ti base metal and the diamond coating [20].

In this work the anodic oxidation of simple carboxylic acids (acetic, formic, oxalic) have been investigated on synthetic diamond film electrodes in acidic medium. These compounds are very resistant to oxidation. In fact acetic acid and formic acid are the final oxidation

† Dedicated to the memory of Daniel Simonsson

products during wet air oxidation [21] (oxidation with air at about 300 °C and 100 atm) and oxalic acid is the final product in ozone oxidation [22].

2. Experimental details

Boron-doped diamond films were grown on conductive p-Si substrates (0.1 Ω cm, Siltronix) via the hot filament chemical vapour deposition technique (HF CVD) [18]. The temperature range of the filament was 2440–2560 °C and that of the substrate was 830 °C. The gas mixture used was 1% methane in dihydrogen containing 1 ppm of trimethylboron. The gas mixture was supplied to the reaction chamber at a flow rate of 5 l min^{-1} giving a growth rate of 0.24 μm h^{-1} for the diamond layer. The diamond film thickness obtained was about 1 μm. This HF CVD process produces a columnar, random textured, polycrystalline films on conductive p-Si substrate (Si/diamond).

Electrochemical measurements were made in a conventional three-electrode cell using a computer controlled EG&G potentiostat model M 273A. Diamond was used as working electrode, Pt as a counter and $Hg/Hg_2SO_4 \cdot K_2SO_4$ as reference electrode (0.64 V vs NHE).

Oxidation of organics was performed in a one-compartment electrolytic flow cell (Figure 1A). Diamond was used as anode and zirconium as cathode, both electrodes being discs (80 mm dia.) of 50 cm^2 geometric area each and with an interelectrode gap of 10 mm. The electrolyte was stored in a 500 mL thermoregulated glass tank and circulated through the electrolytic cell by means of a centrifugal pump (Figure 1B). The flow rate of the electrolyte in the cell was 160 dm^3 h^{-1} and the mass transfer coefficient (determined using the ferri/ferrocyanide couple) was 2×10^{-5} m s^{-1}.

The carboxylic acids and the oxidation products were monitored by HPLC on a Shimadzu series 6, using a Supelcogel H column, with a mobile phase 0.13% phosphoric acid solution at a flow rate of 0.17 ml min^{-1}. The current efficiency for the anodic oxidation of organics during electrolysis was obtained through the measurement of the chemical oxygen demand (COD, Hach Imeth AG). The instantaneous current efficiency was then calculated using the relation:

$$\mathrm{ICE} = \frac{(\mathrm{COD})_t - (\mathrm{COD})_{t+\Delta t}}{8\, I\, \Delta t} \times FV \qquad (1)$$

where $(\mathrm{COD})_t$ and $(\mathrm{COD})_{t+\Delta t}$ are the chemical oxygen demands at times t and $t+\Delta t$, respectively, I is the current (A), F is the faradaic constant, and V the volume of the electrolyte (dm^3).

We have also defined the following global parameters [2–4]:

(i) *Average current efficiency* ($\bar{\eta}$), or the electrochemical oxidation index EOI. From the ICE–time (or ICE–Ah dm^{-3}) curve an average value of the current efficiency can be determined using

$$\bar{\eta} = \frac{\int_0^{\tau} \mathrm{ICE}\, \mathrm{d}t}{\tau} \qquad (2)$$

where τ is the duration of the electrochemical treatment.

(ii) *Electrochemical oxygen demand* (*EOD*). This express the amount of 'electrochemically' formed oxygen used for the oxidation of the organic pollutant. EOD (g dm^{-3}) can be calculated using

$$\mathrm{EOD} = \frac{8\bar{\eta}Q}{F} \qquad (3)$$

where Q is the specific electrical charge passed (Ah dm^{-3}).

(iii) *Degree of oxidation* (X). The degree of oxidation, X, can be calculated using

$$X = \frac{\mathrm{EOD}}{\mathrm{COD}^*} \qquad (4)$$

where the COD^* (g dm^{-3}) is the initial COD value.

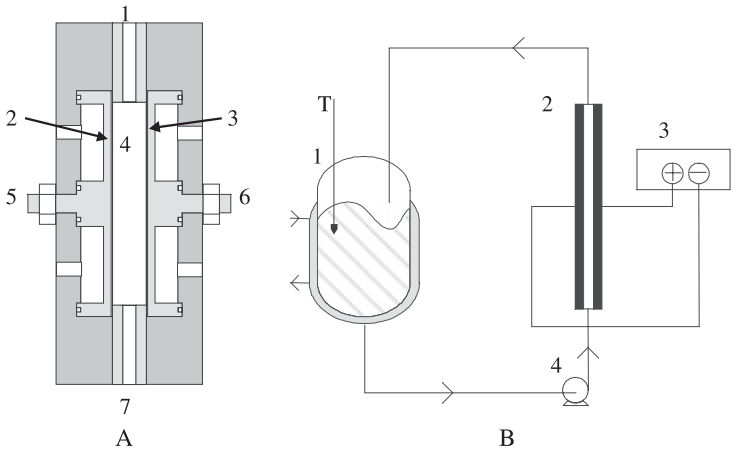

Fig. 1. Set up used for the electrochemical oxidation of carboxylic acids on Si/diamond anodes. (A) electrochemical cell: (1) electrolyte outlet, (2) anode, (3) cathode, (4) electrolyte (5) and (6) electrical connections, (7) electrolyte inlet; (B) equipment used: (1) 0.5 dm^{-3} reactor, (2) electrochemical cell, (3) power supply and (4) recirculation pump.

3. Results and discussion

3.1. *Morphological characterization of the diamond films*

Figure 2 shows a SEM image of polycrystalline films deposited on p-Si. This figure shows that the boron doped diamond layer is continuous and consists of microcrystals randomly arranged. The size of the microcrystals varies from 0.2 to 1 μm and the facets are mainly $\langle 111 \rangle$ oriented with some $\langle 100 \rangle$ orientation.

In the Raman spectra (Figure 3) two sharp peaks (at 1150 nm and 1330 nm) and one broad peak (at 1450–1550 nm) are observed. The first peak at 1150 nm is attributable to the silicon substrate and the second at 1330 nm is due to carbon sp^3 (diamond). The broad peak obtained in the region between 1450 and 1550 nm is due to sp^2 carbon impurities (non-diamond). From the ratio of the diamond to the non-diamond scattering intensity and from the Raman cross-section scattering coefficients for diamond and graphite (i.e., non-diamond carbon) [23] we have found that the non-diamond to the diamond ratio is less than 1%.

3.2. *Electrochemical characterization*

Tafel plots for peroxodisulphate formation [24] and oxygen evolution on diamond in 1 M H_2SO_4 is given in Figure 4. The high value of the obtain Tafel slope (0.23 V decade^{-1}) compared to other classical electrodes (Ti/IrO_2 and Ti/SnO_2–Sb_2O_5 given in the same Figure) [10] are probably due to the semimetal character of the boron doped diamond films and/or due to the formation of oxygen containing functional groups (diamond oxide DO), a poorly defined material, which can act as a barrier for electron transfer. In fact ESCA analysis of the diamond surface show that the O/C ratio increases from 0.08 to 0.22 after anodic polarisation for 30 min at 10 mA cm^{-2}.

The electrochemical activity of diamond films toward the anodic oxidation of simple carboxylic acids was investigated by cyclic voltammetry. A series of voltammograms was determined as a function of the carboxylic acid concentration in 1 M H_2SO_4 at 25 °C. For all studied carboxylic acids, the cyclic voltammograms, recorded below the decomposition potential of water and/or the supporting electrolyte, display no significant change in the presence of acids with respect to the voltammogram for the supporting electrolyte. The only difference in the presence of carboxylic acids is a decrease in the starting potential of water discharge and/or decomposition of the supporting electrolyte. Figures 5 and 6 show typical voltammograms obtained with formic and oxalic acid. For both carboxylic acids the current density at a given potential in the region of decomposition of the supporting electrolyte increases with increasing carboxylic acid concentration. This indicates that the pathway for the oxidation of these carboxylic acids involves intermediates which are formed during decomposition of water and/or the supporting electrolyte.

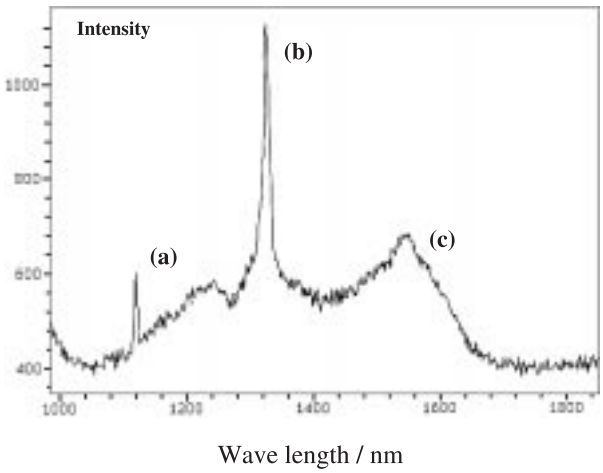

Fig. 3. Raman spectra of the boron doped diamond layer: (a) silicon substrate, (b) sp^3 carbon (diamond) and (c) sp^2 carbon (non-diamond).

3.3. *Anodic oxidation of carboxylic acids*

The anodic oxidation of acetic, formic and oxalic acid were carried out at constant temperature (30 °C) and

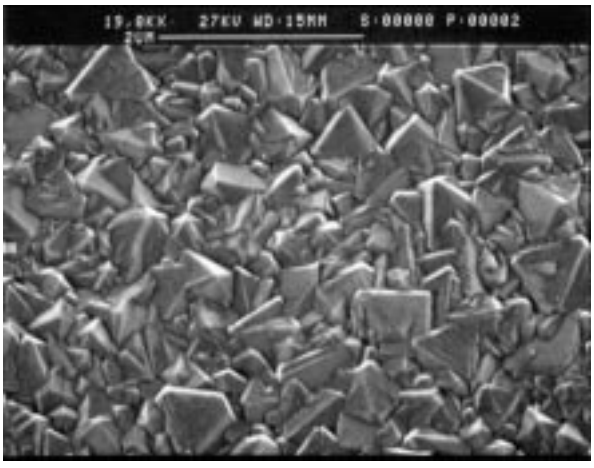

Fig. 2. SEM of boron doped diamond layer deposed on p-Si.

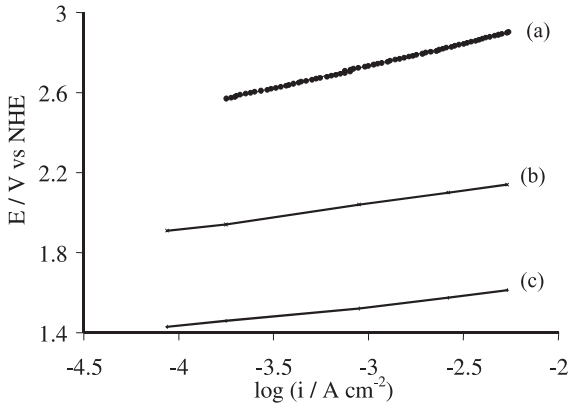

Fig. 4. Tafel plots in 1.0 M H_2SO_4: (a) Si/diamond, (b) SnO_2–Sb_2O_5, (c) IrO_2. $T = 25$ °C.

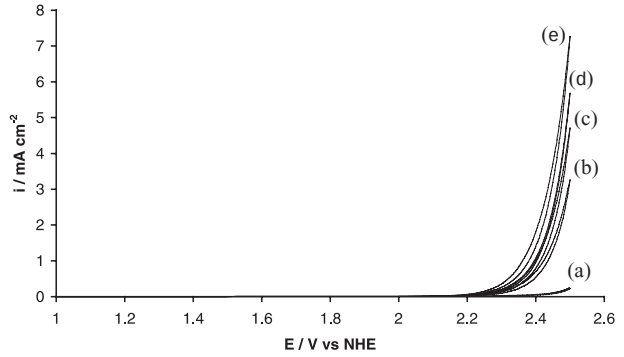

Fig. 5. Cyclic voltammetry on Si/diamond recorded at different formic acid concentrations. Key: (a) 1 M H_2SO_4, (b) 1 M H_2SO_4 + 0.05 M formic acid, (c) 1 M H_2SO_4 + 0.1 M formic acid, (d) 1 M H_2SO_4 + 0.2 M formic acid, (e) 1 M H_2SO_4 + 0.5 M formic acid. Scan rate 50 mV s^{-1}; electrolyte 1 M H_2SO_4; $T = 25\,^{\circ}C$.

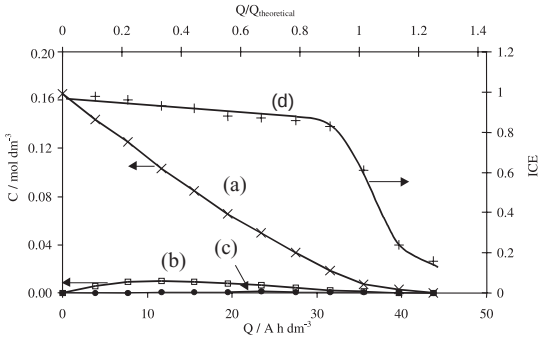

Fig. 7. Evolution of (a) acetic acid (b) formic acid (c) oxalic acid concentrations and (d) ICE during the anodic oxidation of acetic acid solution in 1 M H_2SO_4 on Si/diamond anodes. Anode potential 3.06–3.11 V vs NHE; $i = 30$ mA cm^{-2}; $T = 30\,^{\circ}C$.

under galvanostatic conditions (30 mA cm^{-2}) using the electrolytic cell given in Figure 1. During electrolysis the COD and the concentration of the carboxylic acid and its oxidation products were followed by HPLC.

Figure 7 shows the results obtained with acetic acid. Depending on the degree of oxidation, X (Equation 4), two regions can be distinguished: For $0 < X < 90\%$ the concentration of acetic acid decreases linearly with the specific electrical charge passed (Q) forming mainly CO_2 (Equation 5), small amounts of formic acid and traces of oxalic acid. These acids are further oxidized to CO_2:

$$CH_3COOH + 2\,H_2O \rightarrow 2\,CO_2 + 8\,H^+ + 8\,e^- \qquad (5)$$

In this region the ICE (calculated from Relation 1) decreases linearly from 97% to 85%. For $X > 90\%$ both ICE and the acetic acid concentration decrease exponentially with Q. The rapid decrease in the ICE for $X > 90\%$ is certainly due to the fact that the process is diffusion controlled under these conditions. In fact the acetic acid concentration giving a limiting current corresponding to the electrolysis current (I) can be calculated from the relation:

$$C = \frac{I}{zAFk}$$

where z is the number of electrons exchanged ($Z = 8$ for acetic acid), A the geometric anode surface area (0.005 m^2), k is the mass transfer coefficient ($k = 2 \times 10^{-5}$ m s^{-1}), I the applied current (1.5 A) and F is the faradaic constant.

The value obtained (~20 mM) corresponds to about 90% oxidation of acetic acid which corresponds to the region where the ICE starts to decay exponentially (Figure 7).

Figure 8 shows the influence of applied current density on the variation in acetic acid concentration during electrolysis. Depending on the degree of oxidation (X) two regions can be distinguished: (a) at low degree of conversion ($Q < 20\,Ah\,dm^{-3}$) the oxidation rate of acetic acid is not influenced by the current density within the domain investigated; (b) at high degree of conversion ($Q > 25$ Ah dm^{-3}) the oxidation rate of acetic acid decrease with increasing current density. This behaviour is due to the fact that at high

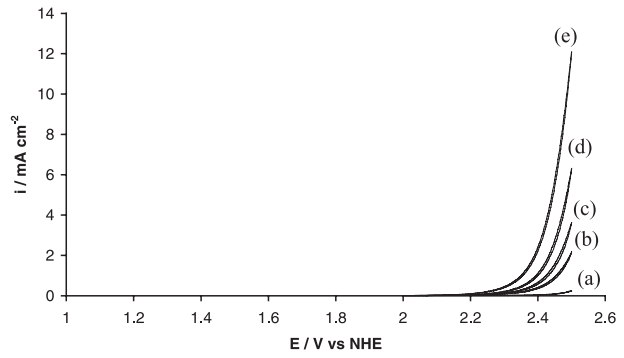

Fig. 6. Cyclic voltammetry on Si/diamond electrodes recorded at different oxalic acid concentrations. Key: (a) 1 M H_2SO_4, (b) 1 M H_2SO_4 + 0.05 M oxalic acid, (c) 1 M H_2SO_4 + 0.1 M oxalic acid, (d) 1 M H_2SO_4 + 0.2 M oxalic acid, (e) 1 M H_2SO_4 + 0.5 M oxalic acid. Scan rate 50 mV s^{-1}; electrolyte 1 M H_2SO_4; $T = 25\,^{\circ}C$.

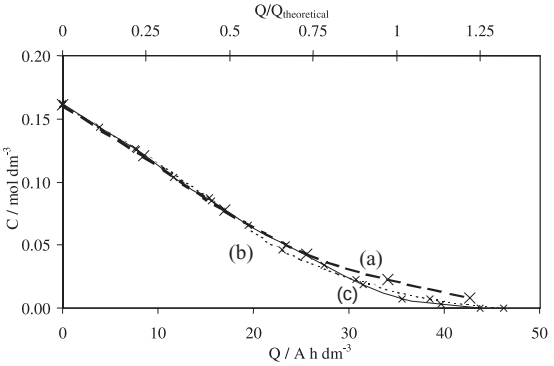

Fig. 8. Evolution of acetic acid concentration during the anodic oxidation of acetic acid solution in 1 M H_2SO_4 on Si/diamond anodes. $T = 30\,^{\circ}C$. Influence of current density (a) 90, (b) 60 and (c) 30 mA cm^{-2}.

Table 1. Anodic oxidation of carboxylic acid solutions in 1 M H_2SO_4 on Si/diamond anodes ($T = 30$ °C, $i = 30$ mA cm^{-2})

	Acetic acid	Formic acid	Oxalic acid
Concentration/mol dm^{-3}	0.165	0.18	0.19
COD*/g dm^{-3}	10.4	2.9	3.0
Q_{th}/A h dm^{-3}	35.0	9.6	10.2
Q/A h dm^{-3}	43.7	12.0	23.5
Q/Q_{th}	1.24	1.25	2.3
EOD/g dm^{-3}	10.1	2.9	3.0
X	0.97	1.0	1.0
Average current efficiency**	0.90	0.90	0.70

** Average current efficiency for $0 < X < 0.9$

degree of conversion the oxidation rate is diffusion controlled and consequently the current efficiency decreases with the applied current density.

The behaviour of the other carboxylic acid investigated is similar to those of acetic acid, both oxalic and formic acid are oxidized to CO_2 (Equations 6 and 7) with a high ICE for $0 < X < 90\%$ then for $X > 90\%$ ICE decrease exponentially with Q.

$$(COOH)_2 \rightarrow 2\,CO_2 + 2\,H^+ + 2\,e^- \quad (6)$$

$$HCOOH \rightarrow CO_2 + 2\,H^+ + 2\,e^- \quad (7)$$

Table 1 shows: the concentration of the carboxylic acid in the electrolyte (1 M H_2SO_4), the initial chemical oxygen demand (COD*), the theoretical specific electrical charge necessary for the complete combustion of the carboxylic acids according to Equations 5–7 (Q_{th}), the effective specific electric charge passed (Q), the electrochemical oxygen demand (EOD), the degree of oxidation (X) and the average current efficiency ($\bar{\eta}$) for $0 < X < 90\%$. This Table shows that the carboxylic acids investigated can be completely oxidised to CO_2 on diamond electrodes with high current efficiency.

All these results show that the doped diamond electrodes behave as a 'non-active' anodes [9, 10]. Oxidation on this type of electrode, in the potential region of decomposition of water and/or the supporting electrolyte, involves the formation of hydroxyl radicals by water discharge (Equation 8), which may be either electrochemically oxidized to dioxygen (Equation 9) or assist in to the complete oxidation of the carboxylic acid (Equation 10):

$$H_2O \rightarrow (OH^\bullet)_{ads} + e^- \quad (8)$$

$$(OH^\bullet)_{ads} \rightarrow \tfrac{1}{2}\,O_2 + H^+ + e^- \quad (9)$$

$$\text{Carboxylic acid} \xrightarrow{(OH^\bullet)_{ads}} CO_2 \quad (10)$$

Other oxidants formed on the diamond surface (peroxodisulphuric acid, O_3) can also participate in the oxidation of the carboxylic acids near the electrode surface and/or in the bulk of the electrolyte. In fact, it was found that during electrolysis of H_2SO_4 solution using boron-doped diamond anodes, peroxodisulphuric acid was the main anodic reaction [23], probably due to the oxidation of H_2SO_4 with the electrogenerated hydroxyl radicals (Equation 11):

$$2\,H_2SO_4 + 2(OH^\bullet)_{ads} \rightarrow H_2S_2O_8 + 2\,H_2O \quad (11)$$

3.4. *Long term electrode stability*

The long term stability of the Si/diamond anodes were investigated by anodic polarization of the electrode under galvanostatic conditions (2 A cm^{-2}) in 1 M H_2SO_4 at 25 °C and recording the anode potential as a function of time.

The duration of the experiment was limited to 1000 h; during this period it was found that the anode potential of the Si/diamond anodes increased slowly from 3.2 to 3.9 V vs NHE. Morphological examination of the electrode after this experiment, compared with the electrode before use, shows no structural change of the diamond layer.

4. Conclusions

(i) Cyclic voltammetry measurements have shown that, in the potential region of water stability, the investigated carboxylic acids are inactive on Si/diamond anodes.

(ii) The Si/diamond electrode behaves as 'non-active' anode involving the formation of hydroxyl radicals in the potential region of water discharge. These hydroxyl radicals oxidize the carboxylic acids to CO_2.

(iii) High current efficiencies for the complete oxidation of simple carboxylic acids can be achieved on Si/diamond anodes

(iv) Long term stability of the Si/diamond anode has not shown any structural change of the anode after 1000 h operation.

References

1. Ch. Comninelis and E. Plattner, *Chimia* **42** (1988) 250.
2. Ch. Comninellis and C. Pulgarin, *J. Appl. Electrochem.* **21** (1991) 703.
3. Ch. Comninellis, *Gas, Wasser, Abwasser.* **11** (1992) 792.
4. Ch. Comninellis and C. Pulgarin, *J. Appl. Electrochem.* **23** (1993) 108.
5. Ch. Comninellis, E. Plattner, C. Seignez, C. Pulgarin and P. Péringer, *Swiss Chem.* **14** (1992) 25.
6. C. Pulgarin, N. Adler and P. Péringer and Ch. Comninellis, *Water Res.* **28** (1994) 887.
7. Ch. Comninellis and A. De Battisti, *J. Chim. Phys.* **93** (1996) 673.
8. Ch. Comninellis, *Electrochim. Acta.* **39** (1994) 1857.
9. O. Simond , V. Schaller and Ch. Comninellis, *Electrochim. Acta.* **42** (1997) 2009.
10. G. Foti, D. Gandini and Ch. Comninellis, *Curr. Top. Electrochem.* **5** (1997) 71.

11. G.M. Swain, A.B. Anderson and J.C. Angus, *MRS Bull.* **9** (1998) 56.
12. N. Vinokur, B. Miller, Y. Avyigal and R. Kolish, *J. Electrochem. Soc.* **146** (1999) 125.
13. R. Ramesham, *J. Mater. Sci.* **34** (1999) 1439.
14. Yu.V. Pleskov, Yu.E. Evstefeeva, M.D. Kvotova and V. Laptev, *Electrochim. Acta.* **44** (1999) 3361.
15. Y. Yano, D.A. Tryk, K. Hashimoto and A. Fujishima, *J. Electrochem. Soc.* **145** (1998) 1870.
16. J.J. Carey, W. Henrietta, C.S. Christ Jr., S.N. Lowery, *US Patent 5 399 247* (1995).
17. W. Haenni, H. Baumann, Ch. Comninellis, D. Gandini, P. Niedermann, A. Perret and N. Skinner, *Diam. Relat. Mater.* **7** (1998) 569.
18. A. Perret, W. Haenni, P. Niedermann, H. Baumann, N. Skinner, Ch. Comninellis and D. Gandini, *Electrochem. Soc. Proc.* **32** (1997) 275.
19. A. Perret, W. Haenni, N. Skinner, X.-M. Tang, Ch. Comninellis, D. Gandini, B. Correa and G. Foti, *Diam. Relat. Mater.* **8** (1999) 820.
20. V. Fisher, D. Gandini, S. Laufer, E. Blank and Ch. Comninellis, *Electrochim. Acta.* **44** (1998) 521.
21. J.P. Taylor and J.C. Neygant, *Can. J. Chem.* **52** (1974) 1925.
22. M. Peleg, *Water Res.* **10** (1976) 361.
23. R. De Clements and G. Swain, *J. Electrochem. Soc.* **144** (1997) 856.
24. P-A. Michaud, E. Mahé, W. Haenni, A. Perret and Ch. Comninellis, *Electrochem. Solid-State Lett.*, in press.